



RESEARCH ARTICLE

The analysis of defects in custom 3D-printed acetabular cups: A comparative study of commercially available implants from six manufacturers

Harry Hothi¹  | Johann Henckel¹ | Sean Bergiers²  | Anna Di Laura¹ | Klaus Schlueter-Brust³ | Alister Hart^{1,2}

¹The Implant Science Centre, The Royal National Orthopaedic Hospital, Stanmore, UK

²Department of Orthopaedics and Musculoskeletal Science, University College London, London, UK

³Department of Orthopaedic Surgery, St. Franziskus Hospital Köln, Köln, Germany

Correspondence

Harry Hothi, The Implant Science Centre, The Royal National Orthopaedic Hospital, Stanmore, Middlesex, HA74LP, UK.
Email: harry.hothi@nhs.net

Abstract

Three-dimensional (3D) printing is used to manufacture custom acetabular cups to treat patients with massive acetabular defects. There is a risk of defects occurring in these, often in the form of structural voids. Our aim was to investigate the presence of voids in commercially available cups. We examined 12, final-production titanium custom acetabular cups, that had been 3D-printed by six manufacturers. We measured their mass, then performed micro-computed tomography (micro-CT) imaging to determine their volume and density. The micro-CT data were examined for the presence of voids. In cups that had voids, we computed (1) the number of voids, (2) their volume and the cup volume fraction, (3) their sphericity, (4) size, and (5) their location. The cups had median mass, volume, and density of 208.5 g, 46,471 mm³, and 4.42 g/cm³, respectively. Five cups were found to contain a median (range) of 90 (58–101) structural voids. The median void volume and cup volume fractions of cups with voids were 5.17 (1.05–17.33) mm³ and 99.983 (99.972–99.998)%, respectively. The median void sphericity and size were 0.47 (0.19–0.65) and 0.64 (0.27–8.82) mm, respectively. Voids were predominantly located adjacent to screw holes, within flanges, and at the transition between design features; these were between 0.17 and 4.66 mm from the cup surfaces. This is the first study to examine defects within final-production 3D-printed custom cups, providing data for regulators, surgeons, and manufacturers about the variability in final print quality. The size, shape, and location of these voids are such that there may be an increased risk of crack initiation from them.

KEYWORDS

acetabular defect, custom implant, micro-CT, three-dimensional printing

This is an open access article under the terms of the Creative Commons Attribution License, which permits use, distribution and reproduction in any medium, provided the original work is properly cited.

© 2022 The Authors. *Journal of Orthopaedic Research*® published by Wiley Periodicals LLC on behalf of Orthopaedic Research Society.

1 | INTRODUCTION

The use of three-dimensional (3D) printing, also known as additive manufacturing, is becoming more common in the manufacture of titanium spine, hip, and knee implants. The clinical rationale is the potential for enhanced bony fixation within highly porous implant surfaces, and the ability to print implants with complex shapes to treat patients with challenging bony anatomies.¹ In hip arthroplasty, 3D printing is increasingly being used to manufacture custom acetabular cups for patients with massive acetabular defects.^{2,3}

Whilst this technology is rapidly being adopted by the orthopedic industry, other industries, such as the aerospace sector, have been more cautious. This is due, in part, to the known risk of structural defects that may occur during the printing process.⁴ These defects most often present as voids within the component but may also be seen as cracks or contamination of the starting metal powder.⁵ The potential impact of defects is a risk of fracture of the printed part, depending on their size and location.⁶

A previous study using micro-computed tomography (micro-CT) imaging has shown that some off-the-shelf 3D-printed acetabular cups contain structural voids.⁷ There is no evidence to suggest that the structural integrity of these cups is compromised and indeed there are no known clinical reports of fractures of these components. It has been shown however that the risk of voids occurring increases

as the complexity of the shape being printed increases⁸; we do not currently know the impact of this on custom acetabular cups that are becoming more widely used.

In this study we examined 12 final-production, custom acetabular cups that had been 3D-printed by six manufacturers. Our aim was to use micro-CT imaging to characterize any void defects that existed within these components.

2 | METHODS

2.1 | Materials

We examined 12 unused, final-production titanium alloy acetabular cups that had been 3D-printed with a custom design to treat patients with large acetabular defects, Figure 1. This implant group consisted of two designs printed by each of the six leading manufacturers of 3D-printed orthopedic implants. Each design was made up of the main acetabular body and at least one flange. All the cups examined had exceeded the 6-month window in which they could be used in the patients they had been designed for.

In this study, each of the six manufacturers was randomly assigned with an identifier between Cup_1 and Cup_6; the two cups from each manufacturer were randomly assigned a label of A or B.

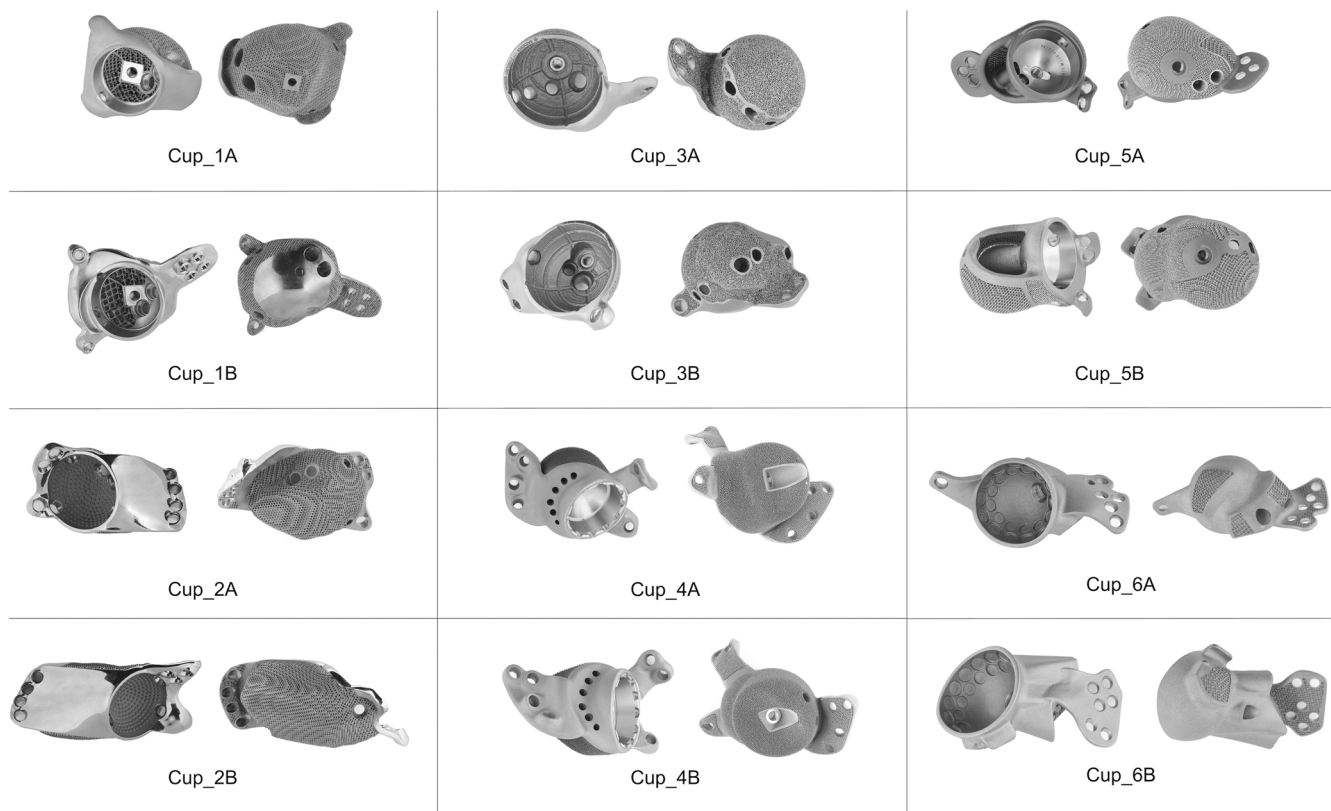


FIGURE 1 Macroscopic images of the 12 cups examined in this study, which were 3D-printed by six manufacturers. Two views of the front and back of each cup are presented.

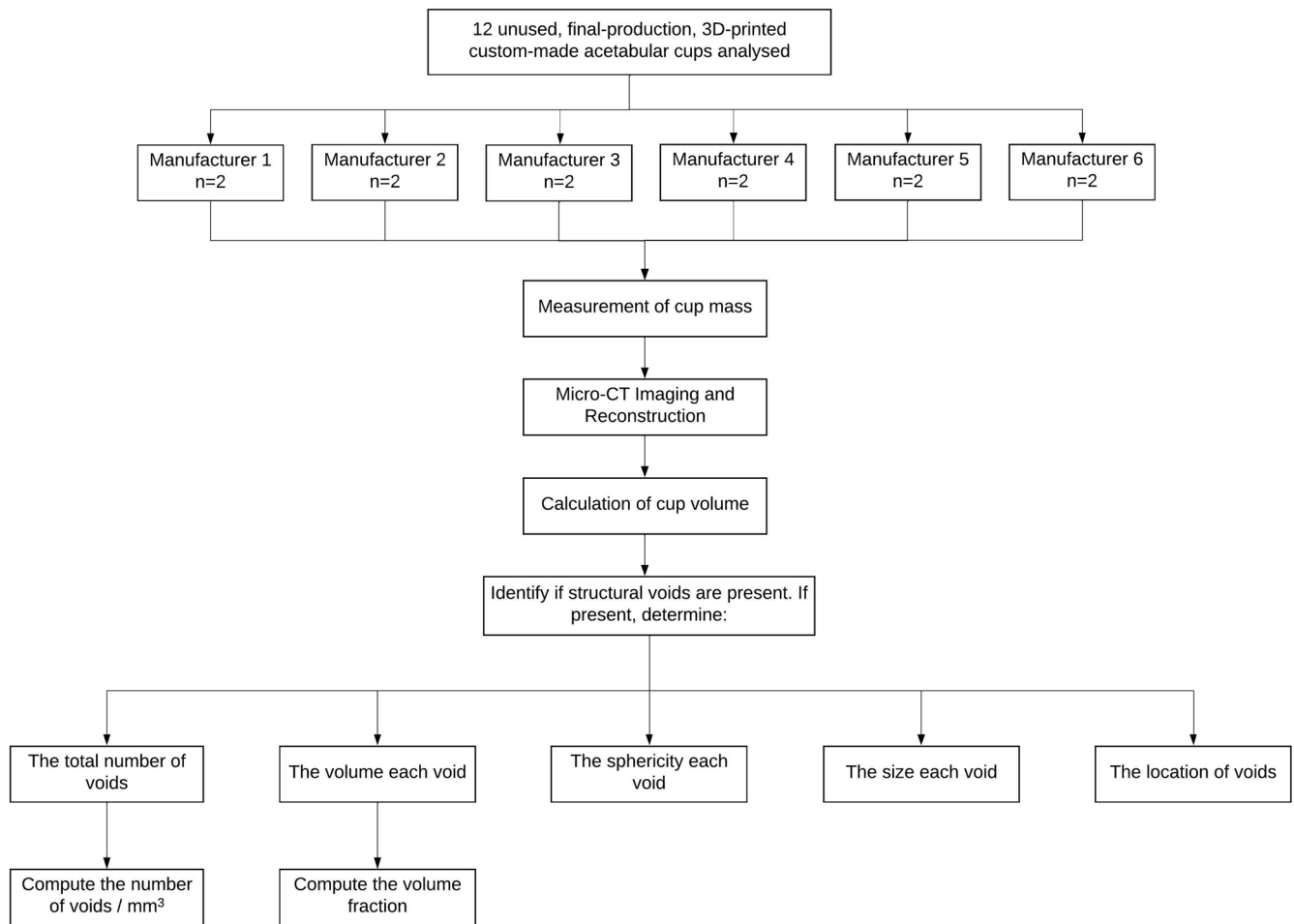


FIGURE 2 Summary of the analysis steps that were performed, in which (a) the final-production 3D-printed implant was obtained, (b) the implant was imaged using a micro-CT scanner and reconstructed in 3D, (c) a void detection algorithm was applied to the 3D reconstruction, (d) the voids were identified and confirmed as likely defects, and (e) the volume, sphericity, size, and location of each void were computed. micro-CT, micro-computed tomography.

From this point on, the implants will be referred to as Cup_1A, Cup_1B, Cup_2A, Cup_2B, and so forth.

The study design is summarized in Figure 2.

2.2 | Cup mass

We measured the mass of each cup using Mettler PC 4400 (Mettler Toledo) digital scales.

2.3 | Micro-CT imaging

We used a Nikon XTH 225 micro-CT scanner (Nikon Metrology) to perform high-resolution 3D imaging of each cup. Scanning was performed with a beam current and voltage of up to 150 μ A and 225 kV, respectively, with the components as close as possible to the beam source whilst still capturing the entire component in the field of view. A 1 mm thick copper filter was positioned at the beam

source to minimize the beam hardening effects that occur when scanning a metal sample. A total of 3177 frames were captured, with an exposure of 1000 ms, in increments of 0.11°.

Figure 3 illustrates the analysis steps performed.

2.4 | Reconstruction of micro-CT data

CT Pro 3D software (Nikon Metrology) was used to reconstruct the two-dimensional (2D) projection images. A filtered back-projection algorithm was utilized, incorporating second-order polynomial-correction numerical filtering to further minimize any beam hardening that may have occurred.

2.5 | Cup volume

The filtered and corrected micro-CT data were imported into the analysis software package Volume Graphics and the cups were

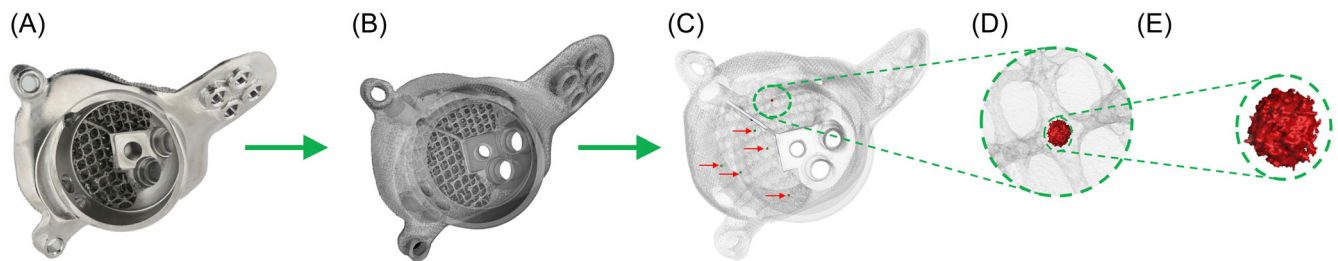


FIGURE 3 Summarizing the study design used [Color figure can be viewed at [wileyonlinelibrary.com](https://onlinelibrary.wiley.com/doi/10.1002/jor.23483)]

segmented using an ISO-50 approach. An automated calculation of the volume of each cup was then performed, before the examination of potential voids within the components.

2.6 | Cup density

A calculation of the density of each cup was made as mass/volume, in which the measure of volume assumed no voids to be present.

2.7 | Void analysis

The Porosity/Inclusion Analysis module within the Volume Graphics software was then used to investigate the presence of any voids within the components, indicating structural defects. The VGDefX algorithm was applied during analysis, in which variations in grayscale values are assessed and compared for each voxel of the scan to determine if the voxel forms part of a void or of the material. An automatic deviation threshold mode was used, with a deviation factor of 0.7 was applied for the standard deviation of the titanium material peak of the gray value distribution. Low noise reduction was applied to the data.

An edge distance calculation was performed for each void that was identified, to determine the minimum distance between the void and the surface of the implant. Following this analysis, the following parameters were obtained for each cup.

2.8 | Number of voids

We recorded the total number of voids that were identified as being likely defects within each component and also calculated the number of voids/mm.³

2.9 | Void volume

We recorded the volume (mm³) of each individual void and the total volume of voids for each cup. We used this to determine the volume fraction, which is a measure of the percentage of material in each cup relative to its volume.

2.10 | Void sphericity

We recorded the sphericity of each void, calculated as a ratio between the surface area of a sphere with the same volume as the void and the surface area of the void itself.

2.11 | Void size

The size (mm) of each void was determined by measuring the diameter of the smallest sphere that could encompass the entire void.

2.12 | Void location

The transparency of the titanium material in each cup was reduced to 90% to better visualize the highlighted voids within the components; these were then inspected to identify their locations. The edge distance calculations were used to report the distance of each void from the cup surface.

3 | RESULTS

We found that Cups 1A, 1B, 3A, 3B, and 5B had evidence of structural defects, presenting as voids within the components. The remaining cups appeared to be free of such voids, Figure 4. Table 1 summarizes all the defect analysis data that were obtained in this study. Figures 5–9 illustrate the cavities that were identified in five out of the 12 cups.

3.1 | Cup mass

The median (range) mass of the cups was 208.5 (133–419) g.

3.2 | Cup volume

The median (range) volume of all cups in this study was 46,471 (30,264–94,864) mm³.

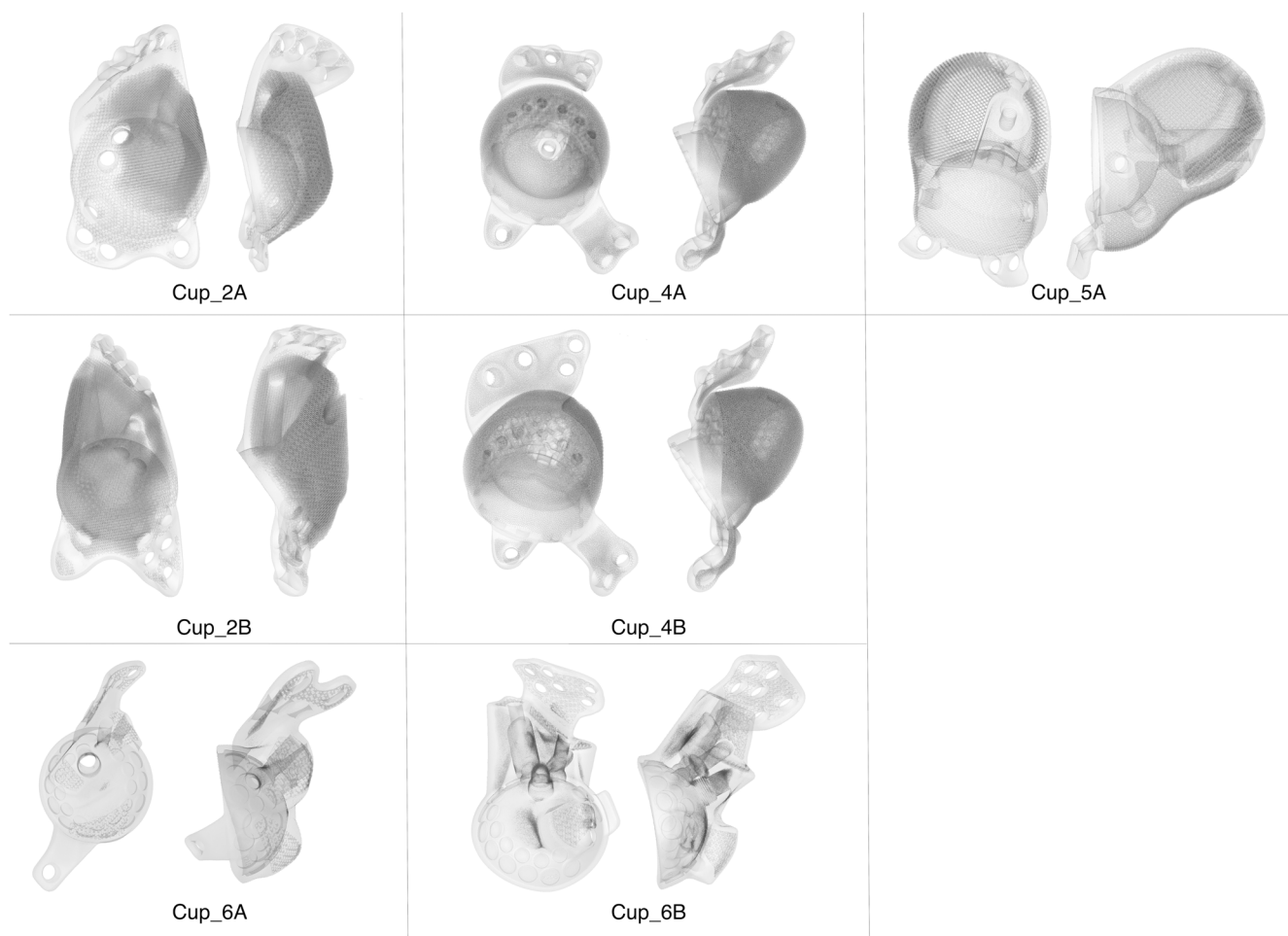


FIGURE 4 Illustrating the 3D reconstructions that were obtained for the cups in which the defect analysis within Volume Graphics did not identify the presence of structural voids

3.3 | Cup density

The median (range) density of the cups was 4.42 (4.27–4.53) g/cm³.

3.4 | Number of voids

The five cups with defects had a median (range) of 90 (58–101) voids, equating to a median of 0.0018 (0.0012–0.0030) voids per mm³.

3.5 | Void volume

The cups with voids were found to have a median volume of 5.17 (1.05–17.33) mm³ of unoccupied space within their internal structures, Figure 10. The median consequential volume fraction in these cups was calculated as 99.983 (99.972–99.998)%, Table 1.

3.6 | Void sphericity

The median sphericity of all voids identified in this study was 0.47 (0.19–0.65), Figure 11.

3.7 | Void size

The median size of all voids in the cups was 0.64 (0.27–8.82) mm, Figure 12. Cups 3B and 5B appeared to have clusters of voids that were interconnected, resulting in voids up to 2.84 and 8.82 mm in the cups, respectively.

3.8 | Void location

The distribution of structural voids in Cups 1A, 1B, 3A, 3B, and 5B is illustrated in Figures 5–9, respectively. Table 1 details the median

TABLE 1 Summary of the defect analysis data obtained for each cup, detailing the presence, and characteristics of structural voids

Cup	Volume of implant (mm ³)	Mass (g)	Density (g/cm ³)	Number of voids	Total volume of voids (mm ³)	Void concentration (defects/mm ³)	Volume fraction (%)	Median (range) void sphericity	Median (range) void size (mm)	Median (range) distance of voids from surface (mm)
1A	50,119	214	4.27	91	1.05	0.0018	99.9979	0.51 (0.24–0.61)	0.41 (0.28–0.78)	0.54 (0.27–1.75)
1B	62,702	269	4.29	101	17.33	0.0016	99.9724	0.48 (0.24–0.61)	0.61 (0.31–2.06)	0.37 (0.17–4.66)
2A	40,387	182	4.51	0	0.00	0.0000	100	-	-	-
2B	94,864	419	4.42	0	0.00	0.0000	100	-	-	-
3A	38,856	176	4.53	87	3.08	0.0000	99.9921	0.46 (0.33–0.65)	0.73 (0.30–1.64)	0.57 (0.19–2.39)
3B	30,264	133	4.39	90	5.17	0.0030	99.9829	0.39 (0.24–0.61)	0.97 (0.29–2.84)	0.50 (0.22–0.83)
4A	46,571	209	4.49	0	0.00	0.0000	100	-	-	-
4B	46,020	208	4.52	0	0.00	0.0000	100	-	-	-
5A	76,498	346	4.52	0	0.00	0.0000	100	-	-	-
5B	46,371	205	4.42	58	8.17	0.0013	99.9824	0.46 (0.19–0.62)	0.79 (0.29–8.82)	0.71 (0.19–2.19)
6A	43,704	193	4.42	0	0.00	0.0000	100	-	-	-
6B	68,246	300	4.40	0	0.00	0.0000	100	-	-	-

Note: Measures of the volume, mass, and density are also presented.

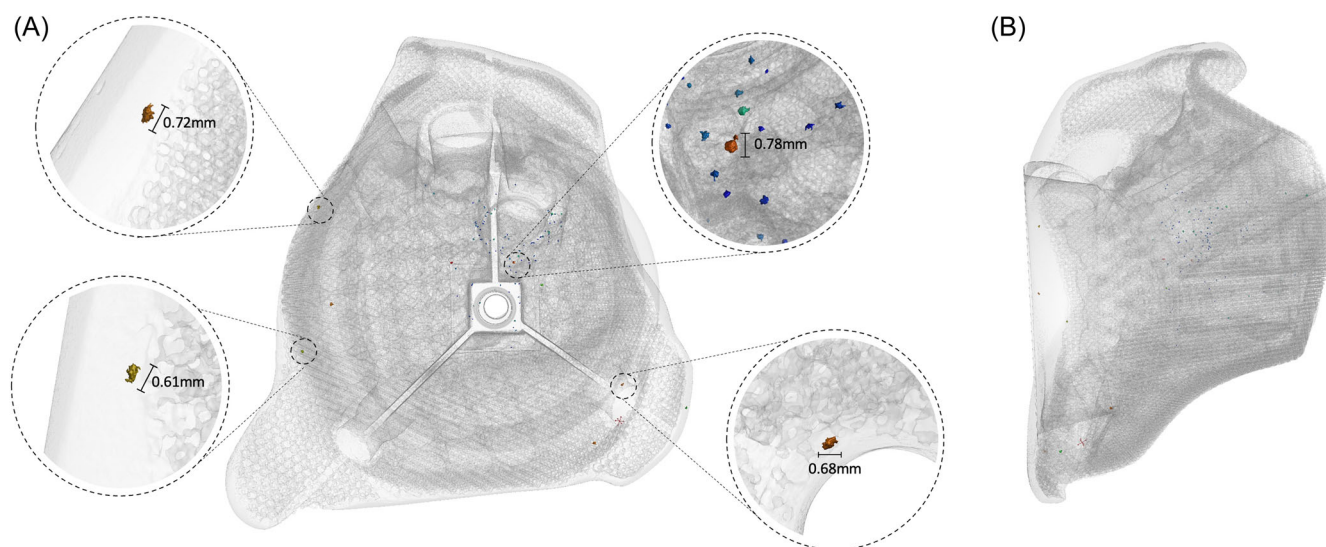


FIGURE 5 Illustrating two views (A, B) of the inverted 3D micro-CT reconstruction of Cup_1A in which 91 structural voids were identified. The voids present are represented by the colored regions and four examples of these have been highlighted, together with their sizes. micro-CT, micro-computed tomography. [Color figure can be viewed at [wileyonlinelibrary.com](https://onlinelibrary.wiley.com/doi/10.1002/jor.25483)]

(range) minimum distance of the voids from the surface of each implant, varying between 0.37 and 0.71 mm.

Across the designs, the majority of voids were situated within (1) the dense column surrounding the central impactor hole, (2) the dense columns of screw holes, (3) the peripheral dense regions of flanges, (4) the transition area between main cup body and flanges, and (5) within the rim of the acetabular opening. The largest connected cluster of voids in this study was observed within Cup_5B, measuring 8.82 mm in length. These were situated at the

transition point between the main body and the “two screw hole” flange.

4 | DISCUSSION

This is the first study to investigate the presence of structural defects within final-production 3D-printed custom acetabular cups. We found that five out of the 12 cups examined had evidence of internal

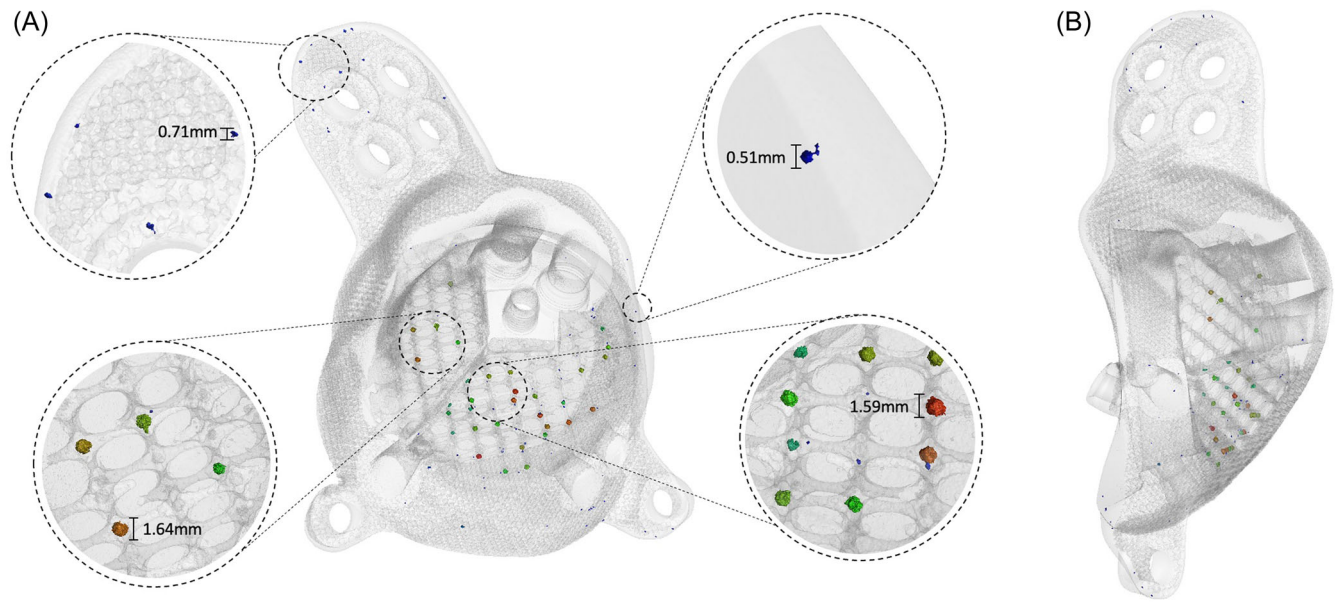


FIGURE 6 Illustrating two views (A, B) of the inverted 3D micro-CT reconstruction of Cup_1B in which 101 structural voids were identified. Examples of four different regions with voids across the cup are highlighted, together with their sizes. micro-CT, micro-computed tomography. [Color figure can be viewed at [wileyonlinelibrary.com](https://onlinelibrary.wiley.com/doi/10.1002/jor.25483)]

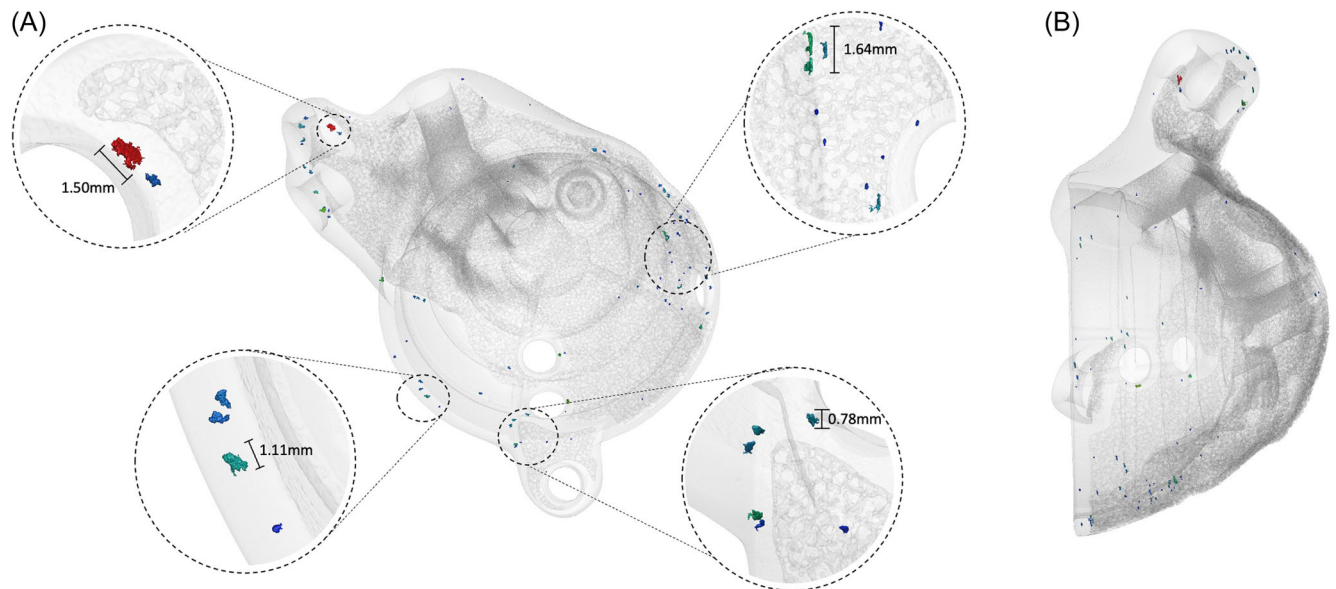


FIGURE 7 Illustrating two views (A, B) of the inverted 3D micro-CT reconstruction of Cup_3A in which 87 structural voids were identified. Examples of four different regions with voids across the cup are highlighted, together with their sizes. micro-CT, micro-computed tomography. [Color figure can be viewed at [wileyonlinelibrary.com](https://onlinelibrary.wiley.com/doi/10.1002/jor.25483)]

voids, ranging between 0.27 and 8.82 mm in size, located between 0.17 and 4.66 mm from their surfaces. The majority of voids were discovered adjacent to screw holes, within flanges, and in regions where there was a transition to a different design feature; at the body-flange connection point and within circumferential grooves in the cup body. This study provides data for regulators, surgeons, and manufacturers about the variability in print quality between designs;

there is opportunity too to understand how these larger voids may be eliminated, as we have seen in some designs.

It is important that the potential impact of the voids found is understood. Previous experimental studies in the aerospace sector have investigated 3D-printed Ti6Al4V samples with volume fractions as high as 99.98%, showing that fatigue cracks can form just under their surfaces under 5 million load cycles, initiated from voids

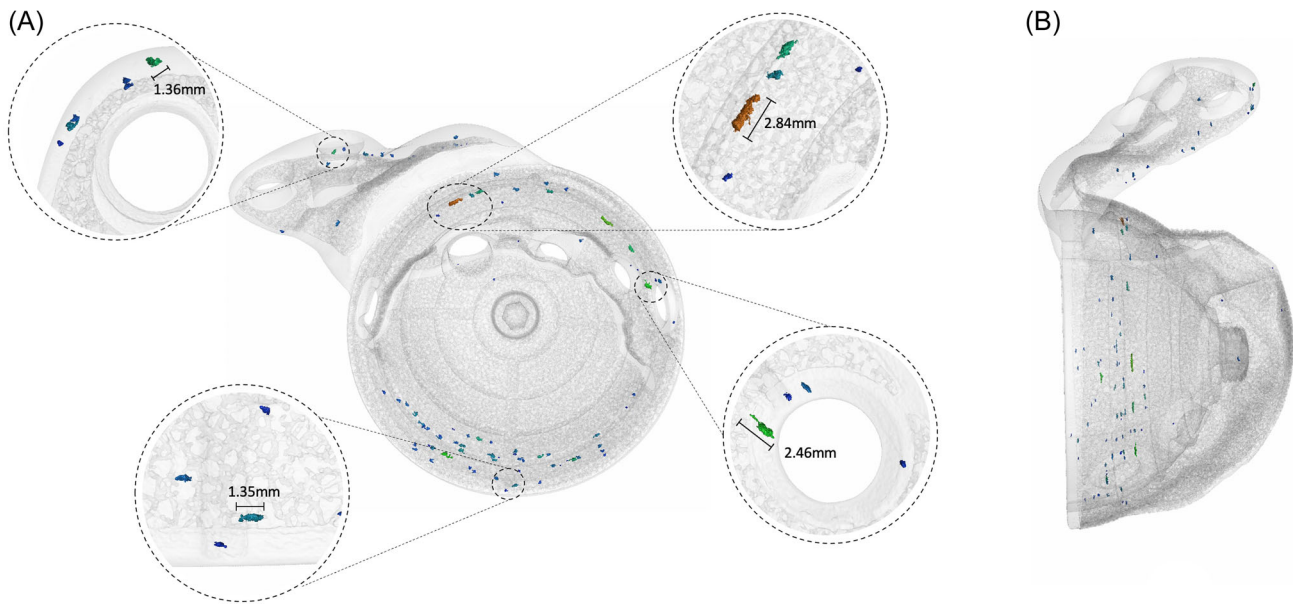


FIGURE 8 Illustrating two views (A, B) of the inverted 3D micro-CT reconstruction of Cup_3B in which 90 structural voids were identified. Examples of four different regions with voids across the cup are highlighted, together with their sizes. There appeared to be clusters of voids that were interconnected, resulting in longer voids up to 2.84 mm in length. micro-CT, micro-computed tomography. [Color figure can be viewed at [wileyonlinelibrary.com](https://onlinelibrary.wiley.com/doi/10.1002/jor.25483)]

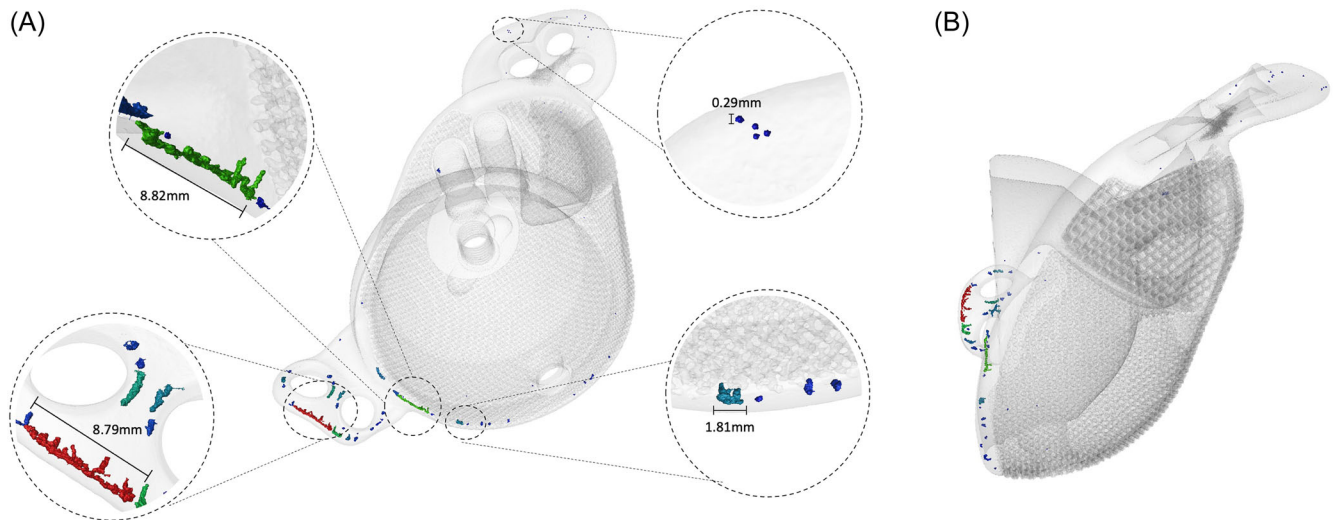


FIGURE 9 Illustrating two views (A, B) of the inverted 3D micro-CT reconstruction of Cup_5B in which 58 separate structural voids were identified. Examples of four different regions with voids across the cup are highlighted, together with their sizes. These include two incidences of the largest connected clusters of voids that were identified in this study, up to a length of 8.82 mm at the transition point between the main cup and body and one of the flanges. micro-CT, micro-computed tomography.

present.⁹ These studies have shown that the most significant factors impacting the fatigue life of a component with structural voids are (in order of descending significance): (1) the location of the void, (2) the size of the void, and (3) its shape.¹⁰

Voids located close to the surface of a component appear to be the most influential in cracks initiating and eventually propagating over time. A recent study performing 1 million load cycle fatigue tests demonstrated that cracks will initiate and propagate in voids located

within 0.1 mm of the surface, even when there are a significantly greater number of larger voids situated deeper within the component.¹¹ Micro-CT scanning of fatigued 3D-printed titanium alloy samples in a different study showed that cracks initiated in voids located within 0.4 mm of their surfaces.¹² Some of the voids identified in our study were as close as 0.17 mm to the surface of the cups, suggesting that they may be within the location in which a risk of crack initiation increases.

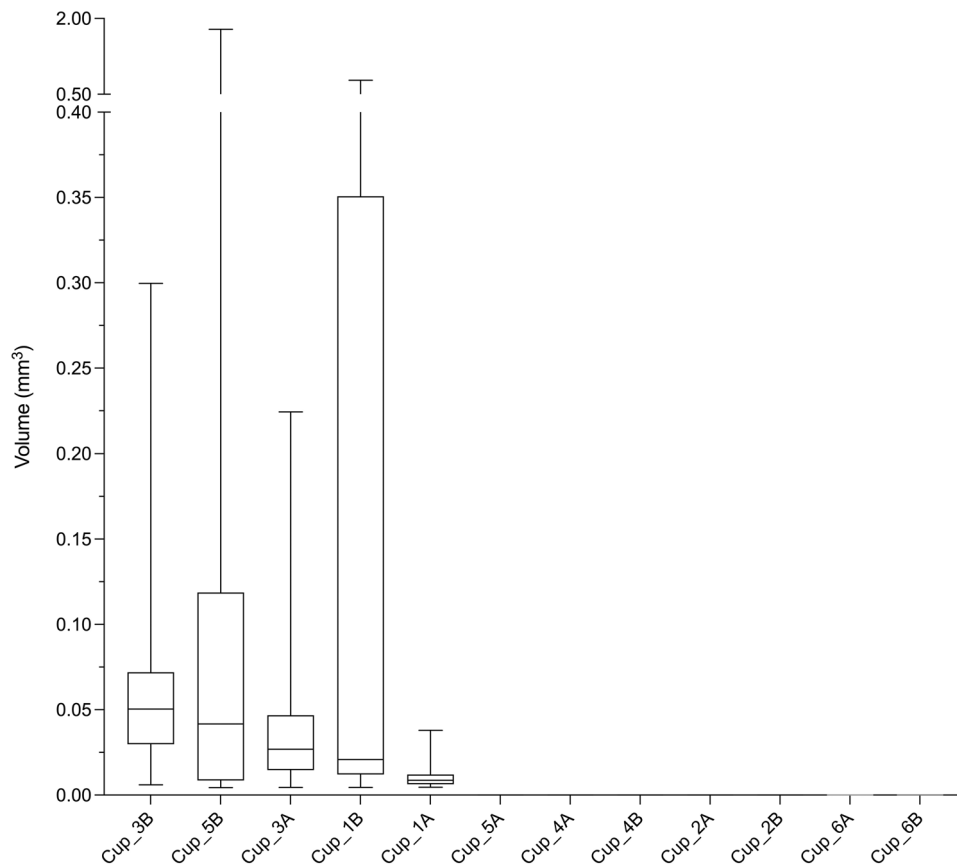


FIGURE 10 Box plots presenting the spread of the volumes of the voids that were present in Cups 1A, 1B, 3A, and 5B, ordered in descending median values. The remaining cups did not have evidence of voids.

The second critical influencing parameter is the size of the void. Unsurprisingly, it has been shown that larger voids increase the risk of fractures occurring and reduce the fatigue life of 3D-printed components.¹³ It has been suggested however that voids below a threshold size in the order of 0.5 mm have a negligible impact on mechanical properties, particularly if they are situated away from the surface.⁸ The median void size of all cups examined was 0.64 mm and the interconnected series of voids in one of the cups resulted in a defect 8.82 mm in length; this was 0.38 mm from the surface at its closest point and raises the question of the impact of structural integrity, particularly given its location at the transition between the main body and flange.

The median sphericity of the voids identified was 0.47 which indicates that were more irregularly shaped rather than being more spherical (i.e., with a sphericity of closer to 1.0). It has been suggested that larger, irregular voids are more prone to stress risers than smaller spherical voids, which may have a negative impact on the mechanical performance of a component.¹⁴ The greatest risk however of a void becoming problematic is reported to occur when a combination of all three detrimental factors relating to location, size, and shape occur.⁸ That is, in circumstances in which large (>0.5 mm), irregularly shaped voids are present within 0.4 mm of the surface of a component. Even in this scenario, the forces and the

cyclical loading that a component is subjected to have to be great enough to exceed the fatigue limits of an implant. The use case of the 3D-printed component in question is an important consideration; there will clearly be differences in the demands placed on a component used in an aircraft (e.g.) and those placed on a hip implant. It may be that a 3D-printed orthopedic implant that contains voids is able to maintain its structural integrity, rather than a 3D-printed component used in an aircraft which may be subjected to considerably greater cyclical loading forces. This may help explain why there have been no incidences of fractures in these 3D-printed implants despite evidence that they do contain voids.

Nevertheless, our study did find that 7 out of the 12 cups examined had no evidence of structural voids that were detectable at the scanning resolution used (i.e., no voids greater than 0.09 mm were detected within these seven cups). The voids that were found in the current study appear to have primarily been formed due to a “lack of fusion,” which results in characteristic irregular-shaped voids that are often larger in size, of the magnitude that we observed. Lack of fusion voids typically occurs when the starting powder particles fail to reach their full melting temperature to appropriately fuse together¹⁵; the reasons for this are multifactorial, including variability of the spot size of the laser, how fast it moves, the power of the laser and the quality of the powder.⁵

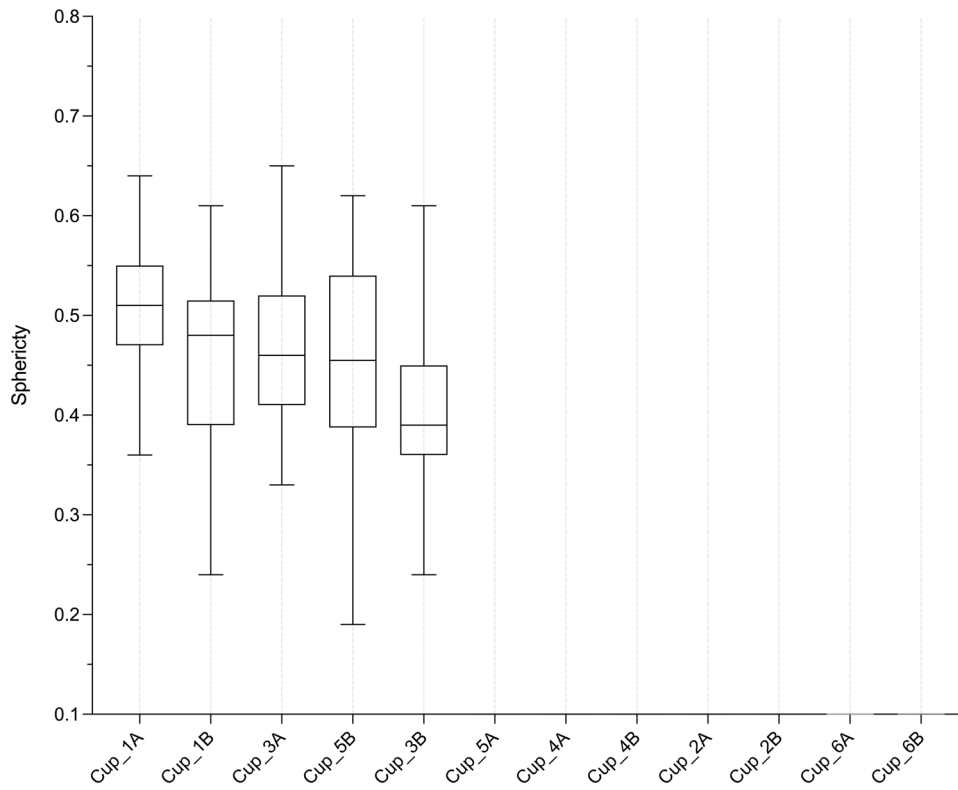


FIGURE 11 Boxes plots of the spread of the sphericity of the voids within the cups, ordered in descending median values.

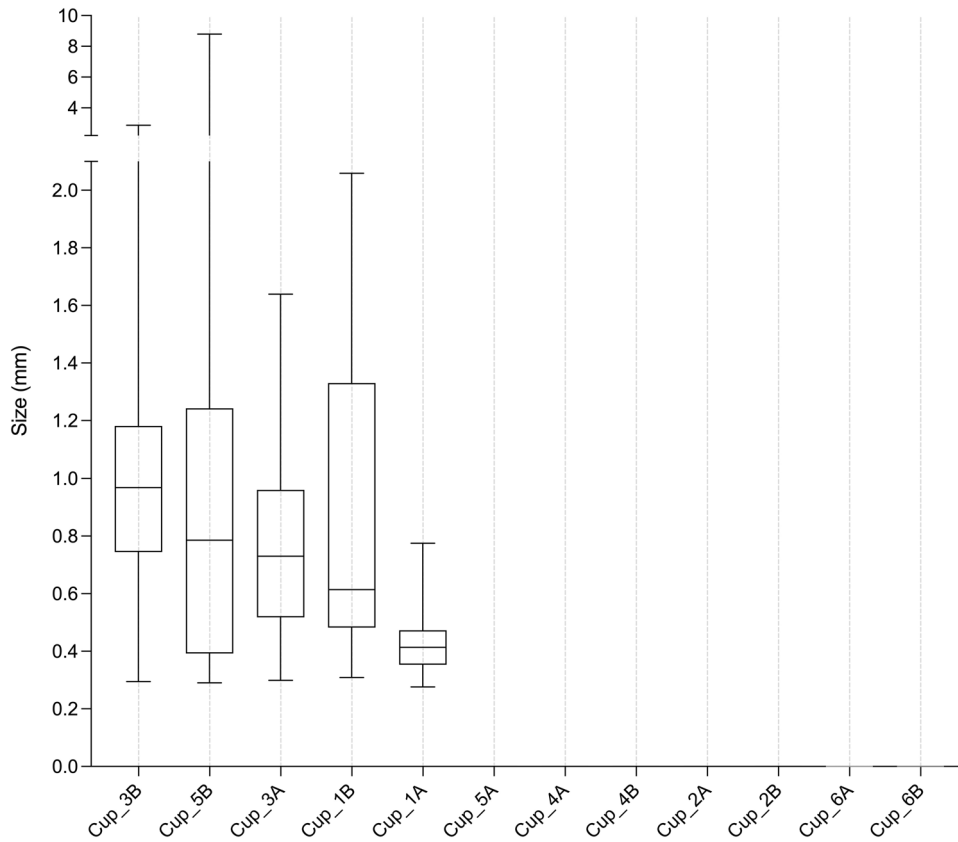


FIGURE 12 Box plots of the size of the spread of the sizes of the voids present within the cups, ordered in descending median values.

All manufacturers utilize postprocessing methods to eliminate voids that may form during the printing process. The most commonly used method is known as hot isostatic pressing (HIP) in which a high-isostatic-pressure gas, usually argon, is applied to the printed part at temperatures high enough to maximize plastic deformation of the material, theoretically leading to internal voids collapsing.¹⁶ Subsequent processes of creep and diffusion lead to voids fully closing and being entirely eliminated. Experimental studies have shown the HIP process to be highly effective at removing large voids within the central regions of printed parts however it has been reported that this method may be less effective at fully eliminating voids closer to the surface.⁸ The findings from our study are consistent with these experimental studies, in which the voids identified were all located a median of 0.5 mm from the implant surfaces. We do not know however the precise postprocessing methods that were used by the different manufacturers and if the absence of voids in some designs was due to a difference in the postprocessing or indeed in the printing process itself.

We acknowledge the limitations of this study. Whilst our micro-CT parameters were optimized to maximize the resolution of the scans, we were not able to detect voids that were smaller than twice the voxel size of the scans (i.e., smaller than $2 \times 0.045 \text{ mm} = 0.09 \text{ mm}$). It may be the case that smaller cavities were present in these cups however, as discussed previously, it has been suggested that these sizes are unlikely to impact the mechanical integrity of 3D-printed components.⁸ Interestingly, the smallest void that we detected was 0.28 mm in size, notably larger than the minimum detectable size. Nevertheless, future studies should seek to understand if smaller cavities are present in these types of implants and involve a greater number of implants to understand the scale of print variability between manufacturers. Future research should also extend to independent mechanical testing of these components to better understand failure mechanisms arising from these voids.

5 | CONCLUSION

This is the first study to examine structural defects within final-production 3D-printed custom acetabular cups. We found evidence of voids in five cups that were between 0.27 and 8.82 mm in size and located between 0.17 and 4.66 mm from their surfaces. The size, shape, and location of these voids are such that there may be an increased risk of crack initiation from them. This study provides data for regulators, surgeons, and manufacturers about the variability in print quality between different designs in relation to eliminating printing defects.

AUTHOR CONTRIBUTIONS

Harry Hothi, Johann Henckel, and Alister Hart contributed to the study design. Harry Hothi, Sean Bergiers, Anna Di Laura, and Klaus

Schlueter-Brust contributed to data acquisition and analysis. Harry Hothi, Johann Henckel, Klaus Schlueter-Brust, and Alister Hart contributed to the interpretation of data. Harry Hothi, Johann Henckel, Sean Bergiers, and Anna Di Laura wrote the first draft of the manuscript. Klaus Schlueter-Brust and Alister Hart edited the manuscript. All authors have read and approved the final submitted manuscript.

ACKNOWLEDGMENTS

There was no funding allocated for this study.

CONFLICTS OF INTEREST

The authors declare no conflicts of interest.

ORCID

Harry Hothi  <http://orcid.org/0000-0001-8745-2111>

Sean Bergiers  <http://orcid.org/0000-0002-7884-7100>

REFERENCES

- Dall'Ava L, Hothi H, Di Laura L, Henckel J, Hart A. 3D printed acetabular cups for total hip arthroplasty: a review article. *Metals*. 2019;9(7):729.
- Durand-Hill M, Henckel J, Di Laura A, Hart AJ. Can custom 3D printed implants successfully reconstruct massive acetabular defects? A 3D-CT assessment. *J Orthop Res*. 2020;38(12):2640-2648.
- Tack P, Victor J, Gemmel P, Annemans L. Do custom 3D-printed revision acetabular implants provide enough value to justify the additional costs? The health-economic comparison of a new porous 3D-printed hip implant for revision arthroplasty of Paprosky type 3B acetabular defects and its closest alternative. *Orthop Traumatol Surgery Res: OTSR*. 2021;107(1):102600.
- Blakey-Milner B, Gradl P, Snedden G, et al. Metal additive manufacturing in aerospace: a review. *Mater Des*. 2021;209:1-33.
- Brennan MC, Keist JS, Palmer TA. Defects in metal additive manufacturing processes. *J Mater Eng Perform*. 2021;30:4808-4818.
- Liu QC, Elambasseril J, Sun SJ, Leary M, Brandt M, Sharp PK. The effect of manufacturing defects on the fatigue behaviour of Ti-6Al-4V specimens fabricated using selective laser melting. *Adv Mater Res*. 2014;891-892:1519-1524.
- Hothi H, Dall'Ava L, Henckel J, et al. Evidence of structural cavities in 3D printed acetabular cups for total hip arthroplasty. *J Biomed Mater Res Part B: Appl Biomater*. 2020;108(5):1779-1789.
- Du Plessis A, Yadroitsava I, Yadroitsev I. Effects of defects on mechanical properties in metal additive manufacturing: a review focusing on X-ray tomography insights. *Mater Des*. 2020;187:108385.
- Malefane LB, Du Preez WB, Maringa M, Du Plessis A. Tensile and high cycle fatigue properties of annealed Ti6Al4V (ELI) specimens produced by direct metal laser sintering, south. *Afr J Ind Eng*. 2018;29:299-311.
- Serrano-Munoz I, Buffière BY, Mokso R, Verdu C, Nadot Y. Location, location & size defects close to surfaces dominate fatigue crack initiation. *Sci Rep*. 2017;7(45239):1-9.
- Andrea O, Pessard E, Koutiri I, et al. A competition between the contour and hatching zones on the high cycle fatigue behaviour of a 316L stainless steel: analyzed using X-ray computed tomography. *Mater Sci Eng A*. 2019;757:146-159.
- Benedetti M, Fontanari V, Bandini M, Zanini F, Carmignato S. Low- and high-cycle fatigue resistance of Ti-6Al-4V ELI additively

- manufactured via selective laser melting: mean stress and defect sensitivity. *Int J Fatigue*. 2018;107:96-109.
13. Du Plessis A, Yadroitsava I, Le Roux SG, et al. Prediction of mechanical performance of Ti6Al4V cast alloy based on microCT-based load simulation. *J Alloys Compd*. 2017;724:267-274.
 14. Hu YN, Wu SC, Withers PJ, et al. The effect of manufacturing defects on the fatigue life of selective laser melted Ti-6Al-4V structures. *Mater Des*. 2020;192:108708.
 15. Vilaro T, Colin C, Bartout JD. As-fabricated and heat-treated microstructures of the Ti-6Al-4V alloy processed by selective laser melting. *Metall Mater Trans A*. 2011;42(10):3190-3199.
 16. Tammis-Williams S, Withers PJ, Todd I, Prangnell PB. The effectiveness of hot isostatic pressing for closing porosity in titanium

parts manufactured by selective electron beam melting. *Metall Mater Trans A*. 2016;47:1939-1946.

How to cite this article: Hothi H, Henckel J, Bergiers S, Di Laura A, Schlueter-Brust K, Hart A. The analysis of defects in custom 3D-printed acetabular cups: a comparative study of commercially available implants from six manufacturers. *J Orthop Res*. 2022;1-12. doi:10.1002/jor.25483